

Resonant properties of a nonlinear dissipative layer excited by a vibrating boundary: Q-factor and frequency response

B. O. Enflo^{a)}

Department of Mechanics, Kungl. Tekniska Högskolan, S-10044 Stockholm, Sweden

C. M. Hedberg^{b)} and O. V. Rudenko^{c)}

Blekinge Institute of Technology, S-371 79 Karlskrona, Sweden

(Received 29 March 2004; revised 19 May 2004; accepted 10 October 2004)

Simplified nonlinear evolution equations describing non-steady-state forced vibrations in an acoustic resonator having one closed end and the other end periodically oscillating are derived. An approach based on a nonlinear functional equation is used. The nonlinear Q-factor and the nonlinear frequency response of the resonator are calculated for steady-state oscillations of both inviscid and dissipative media. The general expression for the mean intensity of the acoustic wave in terms of the characteristic value of a Mathieu function is derived. The process of development of a standing wave is described analytically on the base of exact nonlinear solutions for different laws of periodic motion of the wall. For harmonic excitation the wave profiles are described by Mathieu functions, and their mean energy characteristics by the corresponding eigenvalues. The sawtooth-shaped motion of the boundary leads to a similar process of evolution of the profile, but the solution has a very simple form. Some possibilities to enhance the Q-factor of a nonlinear system by suppression of nonlinear energy losses are discussed. © 2005 Acoustical Society of America.

[DOI: 10.1121/1.1828548]

PACS numbers: 43.25.Gf [MFH]

Pages: 601–612

I. INTRODUCTION

The resonance is known as one of the most interesting phenomena in the physics of vibrations and waves. It manifests itself markedly, if the dependence of the amplitude of a forced oscillation on frequency (i.e., the frequency response) has a sharp maximum. In this case, the ratio of the central frequency ω_0 of the spectral line imaging the response to the characteristic width of this line is large in magnitude. This ratio, known as the Q-factor, can be used as a measure of the “quality” of a resonant system. At large values of Q the system can contain high density of vibrational energy, because the ratio of the steady-state forced oscillation and the external driving force is equal to Q.

For $Q \gg 1$ the approach to the equilibrium state goes on very slowly, because the characteristic relaxation time is about Q/ω_0 . The duration of the increase of the vibration amplitude (or decrease, if the source is shut off) contains a great number of periods which is of the order of Q.

The excitation of strong vibrations in a high-Q system can lead to the appearance of nonlinear effects, the best known example of which is the destruction of the system. On the other hand, high-Q devices are used for the most precise measurements in different branches and applications.

This work is devoted to the analysis of the frequency response and Q-factor of a nonlinear acoustic resonator.

Standing waves are of great interest for nonlinear wave theory and technologies.^{1–3} Using high-Q resonators, it is

possible to accumulate a considerable amount of acoustic energy and provide, in consequence, conditions for clear manifestation of nonlinear phenomena⁴ even in case of a weak power source. Extremely high Q-factor magnitudes, $Q \sim 10^8 - 10^9$, were reached in mechanical resonators designed for the detection of bursts of gravitational waves.⁵ Very strong vibrations were excited in gas-filled resonators of complicated shape, in particular conical or bulb-shaped ones.⁶

At small amplitudes of vibration, the Q-factor is limited by linear absorption caused by dissipative properties of both the medium inside the cavity of the resonator and its boundaries, as well as by radiation losses essential for open resonators. All these types of absorption do not depend on the amplitude. Therefore, for a resonator of given design, the Q-factor is the constant suitable for estimation of its “quality.”

As the amplitude increases, nonlinear phenomena become important. The progressive distortion of the wave profile often leads to formation of shocks which are responsible for additional nonlinear losses. This nonlinear absorption depends on the “strength” of the wave (namely, on its amplitude, peak pressure, intensity, etc.) and can be several orders higher than the usual linear one.³ Consequently, the Q-factor is now determined not only by the design of the nonlinear resonator, but by the strength of the internal acoustic field as well.

The nonlinear Q-factor was earlier evaluated by the rate of dying-down of free standing waves between two rigid walls.⁷ It was also calculated for the forced steady-state vibration in this resonator excited by an external force with the same spatial distribution as the fundamental mode.⁸ However, only wave profiles and spectra were studied in detail for

^{a)}Electronic mail: benflo@mech.kth.se

^{b)}Author to whom correspondence should be addressed. Electronic mail: claes.hedberg@bth.se

^{c)}Also at Department of Acoustics, Faculty of Physics, Moscow State University, 119899 Moscow, Russia.

the most typical statement of the problem, in which one rigid wall of the resonator is immovable, and the other wall oscillates periodically (see, for example, Refs. 2, 9–11). Such principal characteristics of this nonlinear resonator as Q -factor and frequency response have not been adequately explored. Some new findings related to the Q -factor are published in Ref. 12. More comprehensive results are given below.

II. SIMPLIFIED APPROACH AND BASIC NONLINEAR EQUATIONS

Evidently, in a linear one-dimensional system the standing wave can be composed of two plane waves propagating in opposite directions:

$$\Phi(x,t) = \varphi_1\left(t - \frac{x}{c}\right) + \varphi_2\left(t + \frac{x}{c}\right); \quad (1)$$

here Φ is potential of particle velocity $\vec{u} = -\nabla\Phi$, and c is sound velocity. It seems that Chester⁹ was first to use the representation (1) to describe approximately the nonlinear field in the cavity of a resonator. This idea was explained and applied to nonlinear standing waves between rigid immovable walls,^{7,8} where the field is described as the sum (1) of two Riemann or Burgers traveling waves. Each of these waves can be distorted significantly by nonlinear self-action, resulting into the formation of a sawtooth-shaped profile from the initial harmonic one with no contribution from the cross-interaction of two counterpropagating waves. In other words, each wave is distorted by itself during the propagation, but there is no energy exchange between them. The idea of “nonlinear superposition” can be used for any wave field described by different mathematical models (see, for example, Ref. 13). Similar approaches have been used later in many works (see, for example, Refs. 11 and 14). Waveguide modes can also be described by a modification of this approach;¹⁵ the nonlinear Brillouin modes were formed¹⁵ by two strongly distorted waves intersecting at equal angles to the axes of a waveguide.

The idea of “nonlinear superposition” was clearly explained in Ref. 12. In short, the successive approximation solution to any nonlinear model governing the field of cross-sectioning waves contains both resonant and nonresonant parts. After several periods of vibration the nonresonant waves become much weaker than the resonant ones, and cannot participate significantly in nonlinear energy exchange. Each of two cross-sectioning (in particular, counterpropagating) waves generates its higher harmonics, but the cross-interaction process can be neglected if the waves are periodic in time. This conclusion is easily seen to be as valid for periodic waves intersecting at any sufficiently large angles,¹⁵ not necessarily equal to 180° , as for counterpropagating waves in 1D geometry.

After these comments, the approximate solution can be written as the sum of two traveling Riemann waves (for an inviscid fluid):

$$u = u_1 + u_2 \\ = F_1\left(\omega t - \kappa x + \frac{\epsilon}{c^2} \omega x F_1\right) + F_2\left(\omega t + \kappa x + \frac{\epsilon}{c^2} \omega x F_2\right), \quad (2)$$

where $F_{1,2}$ are auxiliary functions describing wave profiles, and ϵ is a nonlinearity parameter.

The solution (2) must satisfy the boundary condition on the immovable wall,

$$u(x=0,t) = 0, \quad (3)$$

and the boundary condition on the vibrating boundary,

$$u(x=L,t) = A \sin \omega t. \quad (4)$$

From (2) and (3) follows $F_1 = -F_2 = F$. The unknown function F must be determined from the second boundary condition (4). This determination reduces (2) to the functional equation

$$F\left(\omega t - \kappa L + \frac{\epsilon}{c} \kappa L F\right) - F\left(\omega t + \kappa L - \frac{\epsilon}{c} \kappa L F\right) = A \sin \omega t. \quad (5)$$

The equation (5) is very complicated and cannot be solved exactly analytically. Nevertheless, it can be simplified for most interesting cases, if the following three conditions are satisfied.

First, the length of the resonator must be small in comparison with the shock formation length:^{3,4}

$$L \ll \frac{c^2}{\epsilon \omega |F|_{\max}}, \quad (6)$$

where $|F|_{\max}$ is the maximum amplitude of the function F .

Second, the frequency ω of vibration of the right-hand boundary must differ slightly from a resonant frequency $n\omega_0$:

$$\kappa L = \pi n + \Delta, \quad \Delta = \pi \frac{\omega - n\omega_0}{\omega_0} \ll 1, \quad (7)$$

where Δ is the discrepancy and $\omega_0 = \pi c/L$ is the frequency of the fundamental eigenmode $n=1$.

Third, the energy influx during one period $2\pi/\omega$ from the vibrating boundary to the resonator must be small in comparison with the accumulated energy; in other words,

$$Q \gg 1. \quad (8)$$

The case of vicinity of the fundamental mode ($n=1$) is now considered. Using the weak nonlinearity condition (6) and formulas (7) with the smallness condition for Δ we replace the left-hand side of Eq. (5) by two terms of its series expansion:

$$F\left(\omega t - \kappa L + \frac{\epsilon}{c} \kappa L F\right) - F\left(\omega t + \kappa L - \frac{\epsilon}{c} \kappa L F\right) \\ = F\left(\omega t - \pi - \Delta + \frac{\epsilon(\pi + \Delta)F}{c}\right) \\ - F\left(\omega t + \pi + \Delta - \frac{\epsilon(\pi + \Delta)F}{c}\right) \\ \approx [F(\omega t - \pi) - F(\omega t + \pi)] \\ - \left(\Delta - \frac{\pi \epsilon F}{c}\right) [F'(\omega t - \pi) + F'(\omega t + \pi)]. \quad (9)$$

Because the right-hand side of Eq. (5) is a periodic function, and the Q -factor is presumed to be large (8), the unknown function F must be quasiperiodic. Therefore, its variation during one period can be replaced in Eq. (9) by the derivative

$$F(\omega t - \pi) - F(\omega t + \pi) \approx -2\pi\mu \frac{\partial F(\omega t + \pi)}{\partial(\mu\omega t)}. \quad (10)$$

Here $\mu \ll 1$ is a small parameter, the physical meaning of which will be clear later. Using (9) and (10) the equation (5) takes the form

$$\mu \frac{\partial F}{\partial(\mu\omega t/\pi)} + \left(\Delta - \frac{\pi\epsilon F}{c} \right) \frac{\partial F(\omega t + \pi)}{\partial(\omega t)} = -\frac{A}{2} \sin \omega t. \quad (11)$$

Introducing new dimensionless variables and constants

$$U = \frac{F}{c}, \quad M = \frac{A}{c}, \quad \xi = \omega t + \pi, \quad T = \frac{\omega t}{\pi}, \quad (12)$$

one can rewrite the simplified evolution equation (11) as

$$\frac{\partial U}{\partial T} + \Delta \frac{\partial U}{\partial \xi} - \pi\epsilon U \frac{\partial U}{\partial \xi} = \frac{M}{2} \sin \xi. \quad (13)$$

The equation (13) was derived earlier¹⁷ to describe the sound excitation by a moving laser beam (see also Refs. 18 and 19); it was named ‘‘inhomogeneous Riemann equation with discrepancy.’’ It should be emphasized that the temporal variables ξ and T are ‘‘fast’’ and ‘‘slow’’ time, respectively. From Eq. (13) it follows that the small parameter μ at the derivative on slow time T can play the role of any small number: Δ , M or $U \sim M$.

The evolution equation (13) can be generalized. The boundary $x=L$ can execute not only harmonic vibration but any periodic one. In this case, the boundary condition (4) must be replaced by

$$u(x=L, t) = Af(\omega t), \quad (14)$$

where f is an arbitrary function with the period 2π . The boundary condition (14) leads to a simplified evolution equation, which differs from (13) in its right-hand side, now equaling

$$-\frac{M}{2} f(\xi - \pi). \quad (15)$$

Next generalization of (13) takes into consideration the effective viscosity, $b \neq 0$. In Ref. 20 an equation similar to (13) and (15) was derived with account for dissipation and finite displacement of the vibrating boundary:

$$\frac{\partial U}{\partial T} + \Delta \frac{\partial U}{\partial \xi} - M\phi(\xi) - D \frac{\partial^2 U}{\partial \xi^2} = \frac{M}{2} \phi'(\xi), \quad (16)$$

where $\phi'(\xi)$ is a periodic function and the dimensionless number D , determining the weak absorption of a wave passing through the length L of a resonator, is defined as

$$D = \frac{b\omega^2 L}{2c^3 \rho} \ll 1. \quad (17)$$

However, the volume nonlinearity ($\epsilon \neq 0$) was not considered in Ref. 20.

The objective of the present work is the simultaneous consideration of effects of dissipation and nonlinearity. Because all the phenomena leading to the progressive distortion of the wave are supposed to be weak, the corresponding terms in the evolution equation must be additive.^{3,16} So, combining Eqs. (13), (15) and (16) we derive

$$\frac{\partial U}{\partial T} + \Delta \frac{\partial U}{\partial \xi} - \pi\epsilon U \frac{\partial U}{\partial \xi} - D \frac{\partial^2 U}{\partial \xi^2} = -\frac{M}{2} f(\xi - \pi). \quad (18)$$

The equation (18) was named ‘‘inhomogeneous Burgers equation.’’²¹ Its main properties were studied in Refs. 21 and 22 in the context of stimulated Brillouin scattering of light by nonlinear hypersonic waves.

III. STEADY-STATE VIBRATIONS

The establishment of a steady-state field in a resonator is a result of competition between energy inflow from a vibrating source and its losses caused by linear dissipation and nonlinear absorption. The equilibrium state reached at $T \rightarrow \infty$ can be described by the ordinary differential equation, obtained by integration of Eq. (18) at $\partial U/\partial T = 0$. The simplest case of periodic sawtooth-shaped motion of boundary is considered first. It corresponds to the right-hand side of (18) being equal to $-(M/2)\xi/\pi$ inside the interval $\pi \leq \xi \leq \pi$ and periodically continued outside. For this case the steady-state equation is

$$D \frac{dU}{d\xi} + \frac{\pi\epsilon}{2} (U^2 - C^2) - \Delta U = \frac{\pi M}{4} \left(\frac{\xi^2}{\pi^2} - \frac{1}{3} \right). \quad (19)$$

The constant C in (19) is an arbitrary constant, which has an important physical meaning. From (19) follows

$$\bar{U}^2 = \frac{1}{2\pi} \int_{-\pi}^{\pi} U^2 d\xi = C^2. \quad (20)$$

Thus the constant C^2 is the normalized intensity of one of two counterpropagating waves. The mean value of U is assumed to be zero:

$$\bar{U} = \frac{1}{2\pi} \int_{-\pi}^{\pi} U d\xi = 0. \quad (21)$$

For negligible weak linear absorption, $D \rightarrow 0$, the solution of the quadratic equation corresponding to Eq. (19) is

$$U = \frac{\Delta}{\pi\epsilon} \pm \sqrt{\left(\frac{\Delta}{\pi\epsilon} \right)^2 + C^2 + \frac{M}{2\epsilon} \left(\frac{\xi^2}{\pi^2} - \frac{1}{3} \right)}. \quad (22)$$

For small Mach numbers, $M \ll 3\Delta^2/\pi^2\epsilon$, the linear solution can be derived from one of the branches of the solution (22), namely from the ‘‘-’’ branch for $\Delta > 0$ and from the ‘‘+’’ branch for $\Delta < 0$:

$$U = -\frac{\pi M}{4|\Delta|} \operatorname{sgn} \Delta \left(\frac{\xi^2}{\pi^2} - \frac{1}{3} \right), \quad C^2 = \bar{U}^2 = \frac{\pi^2 M^2}{180\Delta^2} \ll \frac{M}{3\epsilon}. \quad (23)$$

The inequality in the last member of (23) justifies the neglect of C^2 in the derivation from (22) of the expression for U in the first equation of (23).

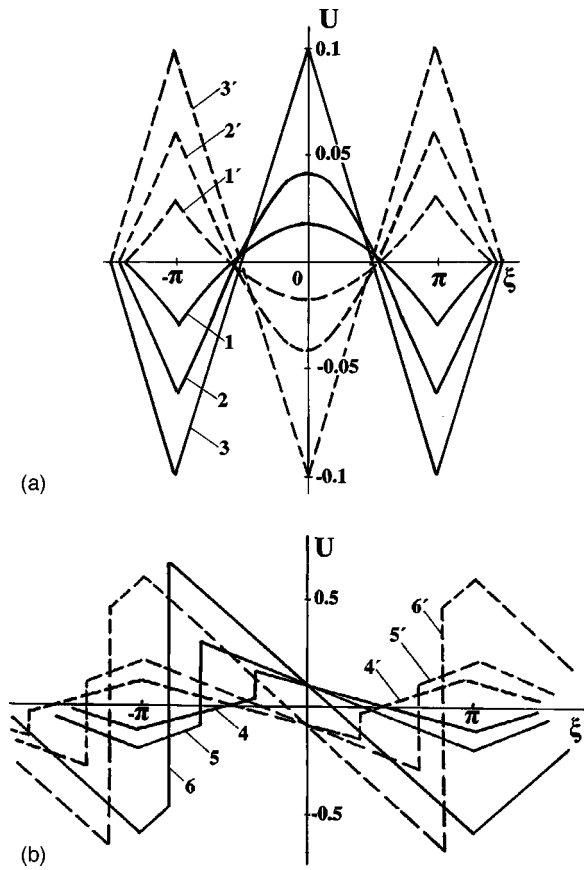


FIG. 1. (a) Temporal profile U of one of two counter-propagating waves forming the steady-state vibration in a nondissipative layer. The dimensionless amplitude $M = A/c$ of the sawtooth-shaped vibration of the boundary is small enough and U does not contain shocks. $(M/2\epsilon) \cdot 10^2$ equals 1, 2.25 and 4 for the curves 1, 2 and 3 correspondingly. (b) The same profiles as in (a) are constructed for greater magnitudes of M . The profiles 4, 5 and 6 corresponding to $(M/2\epsilon) \cdot 10^2 = 4, 9$ and 49 contain shocks.

With increasing M , up to a certain limiting value M_* , which will be determined later, the waveform undergoes progressive nonlinear distortion [Fig. 1(a)], but is still described by one of the branches of the solution (22).

The solid curves 1, 2 and 3 in Fig. 1(a) are constructed for positive discrepancy $\Delta = 0.1\pi\epsilon$, and the dashed curves for the same negative discrepancy. Increase in the number of the curve corresponds to increase in the amplitude of boundary vibration: $10^2(M/2\epsilon) = 1, 2.25$ and 4.

In order to construct curves in Fig. 1(a), the constant C^2 has been determined as a solution of an algebraic eigenvalue problem. The condition (21) applied to (22) leads to the following equation for C^2 :

$$\frac{2\Delta}{\pi\epsilon} = \sqrt{\left(\frac{\Delta}{\pi\epsilon}\right)^2 + C^2} + \frac{M}{3\epsilon} + \frac{(\Delta/\pi\epsilon)^2 + C^2 - M/6\epsilon}{\sqrt{M/2\epsilon}} \times \operatorname{arsinh} \frac{\sqrt{M/2\epsilon}}{\sqrt{(\Delta/\pi\epsilon)^2 + C^2 - M/6\epsilon}}. \quad (24)$$

Maximum value $M = M_*$ at which Eq. (24) has a real solution $C = \Delta/(\sqrt{3}\pi\epsilon)$ is determined by the condition

$$\sqrt{\frac{M}{2\epsilon}} = \frac{2|\Delta|}{\pi\epsilon}, \quad M = \frac{8}{\pi^2\epsilon} \Delta^2 \equiv M_*. \quad (25)$$

At $M = M_*$ the bifurcation happens, and the steady-state waveform becomes discontinuous. The shock front appears at each period of the wave, connecting the two branches of solution (22).

Let the solution U at the moment ξ_0 lie on the “minus” branch of (22). With increasing time $\xi > \xi_0$ the solution must jump to the “plus” branch; otherwise the condition $\bar{U} = 0$ cannot be satisfied. The moment $\xi = \xi_{SH}$ of the jump corresponds to the position of a shock of compression. However, the shock of rarefaction is prohibited in usual media with quadratic nonlinearity, where the velocity of propagation increases with increasing magnitude of the disturbance.²⁴ Therefore, both branches of the solution (22) must have one common point in each period. If and only if the common point exists, the transition can go on in the opposite direction, from the “+” to the “-” branch, without jump.

The common point exists if the expression under the square root in (22) is equal to zero, or

$$C^2 = \frac{M}{6\epsilon} - \left(\frac{\Delta}{\pi\epsilon}\right)^2. \quad (26)$$

For given eigenvalue (26) the solution (22) reduces to

$$U = \frac{\Delta}{\pi\epsilon} \pm \sqrt{\frac{M}{2\epsilon}} \left| \frac{\xi}{\pi} \right|. \quad (27)$$

In order to determine the position of the shock in the wave profile it is necessary to apply the condition $\bar{U} = 0$ to the solution (27):

$$\int_{-\pi}^{\xi_{SH}} \left(\frac{\Delta}{\pi\epsilon} + \sqrt{\frac{M}{2\epsilon}} \frac{\xi}{\pi} \right) d\xi + \int_{\xi_{SH}}^{\pi} \left(\frac{\Delta}{\pi\epsilon} - \sqrt{\frac{M}{2\epsilon}} \frac{\xi}{\pi} \right) d\xi = 0. \quad (28)$$

From the condition (28) follows

$$\xi_{SH} = -\pi \sqrt{1 - \frac{2\Delta}{\pi} \sqrt{\frac{2}{\epsilon M}}}. \quad (29)$$

The equation (29) is valid for the condition $M \geq M_*$ [cf. (25)].

The solution (27), with account for Eq. (29) defining the position of the shock, is shown in Fig. 1(b), which is a continuation of Fig. 1(a) for greater Mach numbers. With increasing $M > M_*$, the shock appearing initially at $\xi = 0$ moves to the position $\xi = -\pi$ (for $\Delta > 0$), which can be reached only at $M \rightarrow \infty$ [cf. (29)]. The solid curves 4, 5 and 6 in Fig. 1(b) are constructed for $10^2(M/2\epsilon) = 4, 9$ and 49 correspondingly.

The dashed curves in Fig. 1(b) demonstrate a similar behavior of the wave profile at equal negative discrepancy $\Delta = -0.1\pi\epsilon$. In this case the shock appears at $M = M_*$ in the point $\xi = 0$ and moves to the point $\xi = \pi$ for $M \rightarrow \infty$.

In Fig. 2 the nonlinear frequency response is given. The curves 1–3 are constructed for different Mach numbers $(M/2\epsilon) = 0.25, 1$ and 2.25 and demonstrate the dependence of $C = \sqrt{U^2}$ on the discrepancy (7) from the resonant frequency ω_0 . Straight lines

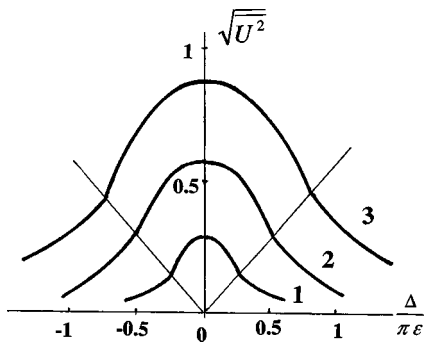


FIG. 2. Nonlinear frequency response defined as rms normalized particle velocity. Curves 1–3 are constructed for different amplitudes of boundary vibration ($M/2\epsilon = 0.25, 1$ and 2.25).

$$\sqrt{U^2} = \frac{1}{\sqrt{3}} \frac{\Delta}{\pi\epsilon} \quad (30)$$

are separatrixes. Below these lines the curves in Fig. 2 are constructed by the solution (22) and (24) for wave profiles which do not contain the shocks. Exactly on the lines (30) the Mach number M is equal to M_* and the transition to the discontinuous solution takes place. So, above the lines (30) another solution [Eq. (27)] was used for calculation of the frequency response.

The frequency response is analyzed not for the dependence of the amplitude on frequency, as is customary for linear vibration, but for the root-mean-square (rms) particle velocity $\sqrt{U^2}$. Because of the fact that the acoustic field U contains a great number of harmonics, the usual definition of frequency response is meaningless.

However, by analogy with the use of frequency response in the evaluation of the Q -factor of a linear resonator, it is possible to evaluate the Q -factor of a nonlinear resonator. As for the linear oscillator, the Q -factor can be defined in two ways: (1) as the ratio between amplitudes of internal and external (driving) vibrations at resonance ($\Delta = 0$) and (2) as a ratio between the resonant frequency and the spectral width of the frequency response. The first way leads to the calculation, using (12) and (26),

$$Q_{NL} = \frac{c(\sqrt{U^2})_{\Delta=0}}{A} = \frac{c}{A} \sqrt{\frac{M}{6\epsilon}} = \frac{1}{\sqrt{6\epsilon M}}. \quad (31)$$

The second way uses the definition of Δ in (7) and the result (25):

$$Q_{NL} = \frac{1}{\Delta} = \frac{2\sqrt{2}}{\pi} \frac{1}{\sqrt{\epsilon M}}, \quad (32)$$

which differs slightly from (31). The nonlinear Q -factor Q_{NL} thus is proportional to $(\epsilon M)^{-1/2}$ with a coefficient $O(1)$ depending on the definition.

For the amplitude of the vibration of the boundary $A = 10$ cm/s the nonlinear evaluation (31) gives for gaseous media $Q \approx 20$. This value is much lower than the value of the linear Q -factor, which is in this case

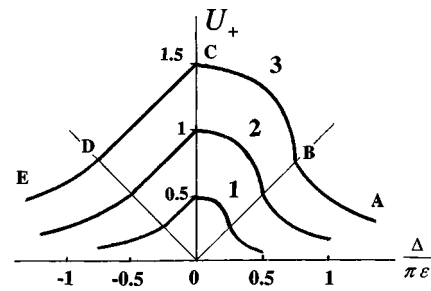


FIG. 3. Nonlinear frequency response defined as positive peak particle velocity on the wave profiles shown in Fig. 1. The boundary vibration amplitude $M/2\epsilon$ equals to 0.25, 1 and 2.25 for curves 1, 2 and 3 respectively.

$$Q = \frac{1}{2\sqrt{2}D} = \frac{c^3\rho}{\sqrt{2}b\omega_0L} = \frac{c^2\rho}{\sqrt{2}\pi b\omega_0}, \quad (33)$$

depending on the effective viscosity b and the resonance frequency $\omega_0 = \pi c/L$. For air-filled resonators at typical frequencies about several kHz the linear evaluation (33) gives $Q \approx 10^3 - 10^4$.

The dependence of the rms velocity $\sqrt{U^2}$ on the discrepancy Δ shown in Fig. 2 is not the only possible definition of nonlinear frequency response. For example, the dependence $U_+(\Delta)$, where U_+ is the positive peak value of U , is also important. This response is shown in Fig. 3 by solid curves for the three values of $M/2\epsilon$ equal to 0.25, 1 and 2.25. The analytical expressions of the sections AB, BC, CD and DE of each curve are different. Namely, U_+ equals to

$$\begin{aligned} \frac{\Delta}{\pi\epsilon} - \sqrt{\left(\frac{\Delta}{\pi\epsilon}\right)^2 + C^2 - \frac{M}{6\epsilon}} & \quad (\text{AB}), \\ \frac{\Delta}{\pi\epsilon} + \sqrt{\frac{M}{2\epsilon} - 2\frac{\Delta}{\pi\epsilon}\sqrt{\frac{M}{2\epsilon}}} & \quad (\text{BC}), \\ -\frac{|\Delta|}{\pi\epsilon} + \sqrt{\frac{M}{2\epsilon}} & \quad (\text{CD}), \\ -\frac{|\Delta|}{\pi\epsilon} + \sqrt{\left(\frac{\Delta}{\pi\epsilon}\right)^2 + C^2 + \frac{M}{3\epsilon}} & \quad (\text{DE}). \end{aligned} \quad (34)$$

Here the eigenvalue C^2 is determined by Eq. (24)

The straight lines 1 and 2 are the same separatrixes as in Fig. 2. Note that U_+ is placed on the top of the shock front only for the section BC; for the other three sections U_+ belongs to smooth portions of the wave profile.

The next important case corresponds to the ordinary differential equation like (19), and with $f = \sin \xi$, i.e., harmonic vibration of the boundary:

$$D \frac{dU}{d\xi} + \frac{\pi\epsilon}{2} (U^2 - C^2) - \Delta U = \frac{M}{2} \cos \xi. \quad (35)$$

Wave profiles for this case were constructed in Ref. 12, but frequency response was not considered there. To understand the behavior at curves in Figs. 5 and 6, it is necessary to give auxiliary formulas using the notations of the present article.

For negligible weak linear absorption, $D \rightarrow 0$, the solution of the quadratic equation corresponding to Eq. (35) is

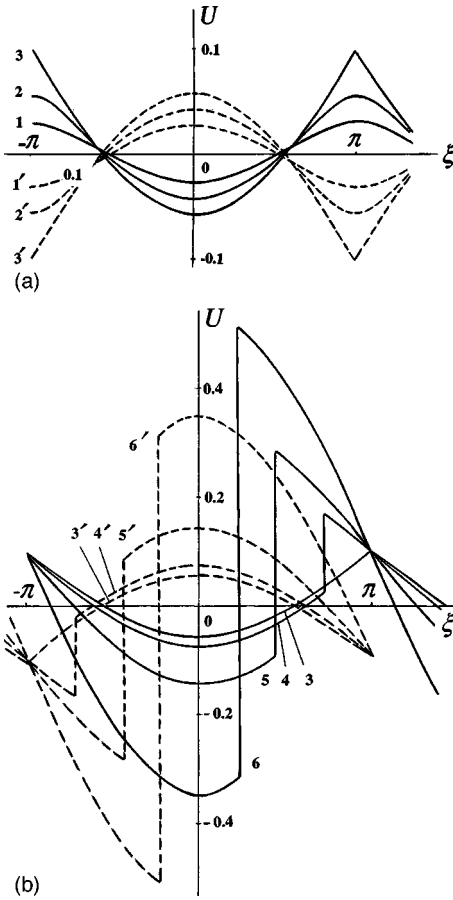


FIG. 4. (a) Temporal profile U of one of two counter-propagating waves forming the steady-state vibration in a nondissipative layer. The dimensionless amplitude $M = A/c$ of the harmonic vibration of the boundary is small enough and U does not contain shocks. $(M/\pi\epsilon) \cdot 10^3$ equals 5.6, 9.1 and 12.3 for the curves 1, 2 and 3 correspondingly. (b) The same profiles as in (a) are constructed for greater magnitudes of M . The profiles 4, 5 and 6 corresponding to $(M/\pi\epsilon) \cdot 10^2 = 1.5, 3$ and 10 contain shocks.

$$U = \frac{\Delta}{\pi\epsilon} \pm \sqrt{\left(\frac{\Delta}{\pi\epsilon}\right)^2 + C^2 + \frac{M}{\pi\epsilon}} \cos \xi. \quad (36)$$

For small Mach numbers, $M \ll \Delta^2/\pi\epsilon$, the linear solution is

$$U = -\frac{M}{2|\Delta|} \operatorname{sgn} \Delta \cos \xi, \quad C^2 = \overline{U^2} = \frac{M^2}{8\Delta^2} \ll \frac{M}{\pi\epsilon}. \quad (37)$$

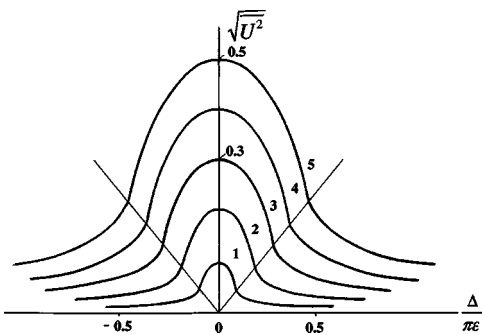


FIG. 5. Nonlinear frequency response defined as rms normalized particle velocity. Curves 1–5 are constructed for different amplitudes of boundary vibration $[(M/\pi\epsilon) \cdot 10^2 = 1, 4, 9, 16$ and 25].

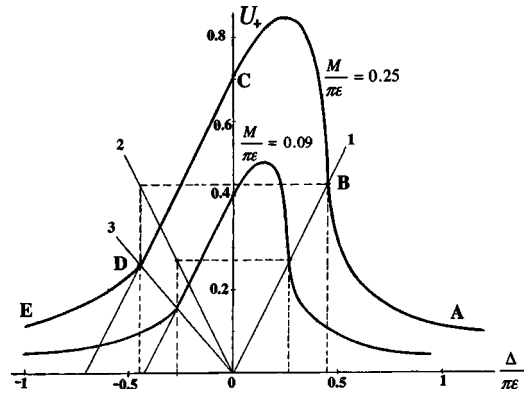


FIG. 6. Nonlinear frequency response defined as positive peak particle velocity on the wave profiles shown in Fig. 4. The boundary vibration amplitude $M/\pi\epsilon$ equals 0.09 and 0.25.

With increasing M the waveform undergoes progressive nonlinear distortion [Fig. 4(a)], but is still described by one of the branches of the solution (36).

The solid curves 1, 2 and 3 in Fig. 4(a) are constructed for positive discrepancy $\Delta = 0.1\pi\epsilon$, and the dashed curves for the same negative discrepancy. Increase in the number of the curve corresponds to increase in the amplitude of boundary vibration: $10^3(M/\pi\epsilon) = 5.6, 9.1$ and 12.3.

In order to construct curves in Fig. 4(a), the constant C^2 has been determined as a solution of an algebraic eigenvalue problem. The condition (21) applied to (36) leads to the following equation for C^2 :

$$\frac{\Delta}{\pi\epsilon} = \frac{2}{\pi} \sqrt{\left(\frac{\Delta}{\pi\epsilon}\right)^2 + C^2 + \frac{M}{\pi\epsilon}} \times E\left(\frac{2M/\pi\epsilon}{\sqrt{(\Delta/\pi\epsilon)^2 + C^2 + M/\pi\epsilon}}\right). \quad (38)$$

Here $E()$ is the complete elliptic integral of the second kind.²³

The solution of Eq. (38) can be written in parametric form:

$$C^2 = \frac{M}{\pi\epsilon} \left[\frac{2}{m} - 1 - \frac{8}{\pi^2} \frac{E^2(m)}{m} \right],$$

$$\frac{\Delta}{\pi\epsilon} = \pm \frac{2\sqrt{2}}{\pi} \sqrt{\frac{M}{\pi\epsilon}} \frac{E(m)}{\sqrt{m}}, \quad (39)$$

where m is a parameter. The argument m of the function $E(m)$ is defined in the region $0 \leq m \leq 1$.²³ From (38) follows that the corresponding region for the discrepancy Δ is given by

$$\frac{2\sqrt{2}}{\pi} \sqrt{\frac{M}{\pi\epsilon}} \leq \frac{|\Delta|}{\pi\epsilon} < \infty \Rightarrow M \leq \frac{\pi}{8\epsilon} \Delta^2 \equiv M_*. \quad (40)$$

At $M = M_*$ the bifurcation happens, and the steady-state waveform becomes discontinuous. The shock front appears at each period of the wave, connecting the two branches of solution (36).

For a discontinuous wave

$$C^2 = \frac{M}{\pi\epsilon} - \left(\frac{\Delta}{\pi\epsilon}\right)^2. \quad (41)$$

For a given eigenvalue (41) the solution (36) reduces to

$$U = \frac{\Delta}{\pi\epsilon} \pm \sqrt{\frac{2M}{\pi\epsilon}} \left| \cos \frac{\xi}{2} \right|. \quad (42)$$

The shock front position ξ_{SH} , determined by the condition $\bar{U}=0$, satisfies the equation

$$\sin\left(\frac{\xi_{SH}}{2}\right) = \frac{\Delta}{2} \sqrt{\frac{\pi}{2\epsilon M}}. \quad (43)$$

From (43) we find that the condition $|\sin(\xi_{SH}/2)| \leq 1$ is equivalent with the condition $M \geq M_*$ [cf. (40)].

The solution (42), with account for Eq. (43) defining the position of the shock, is shown in Fig. 4(b), which is a continuation of Fig. 4(a) for greater Mach numbers. The curve 3 in Fig. 4(b), corresponding to $M = M_*$, is the same as the curve 3 in Fig. 4(a). With increasing $M > M_*$, the shock appearing initially at $\xi = \pi$ (for $\Delta > 0$) moves to the position $\xi = 0$, which can be reached only at $M \rightarrow \infty$ [cf. (43)]. The solid curves 4, 5 and 6 in Fig. 4(b) are constructed for $10^2(M/\pi\epsilon) = 1.5, 3$ and 10 correspondingly.

The dashed curves in Fig. 4(b) demonstrate similar behavior of the wave profile at equal negative discrepancy $\Delta = -0.1\pi\epsilon$. In this case the shock appears at $M = M_*$ in the point $\xi = -\pi$ and moves to the point $\xi = 0$ for $M \rightarrow \infty$.

In Fig. 5 the nonlinear frequency response is given. The curves 1–5 are constructed for different Mach numbers $10^2(M/\pi\epsilon) = 1, 4, 9, 16$ and 25 , and demonstrate the dependence of $C = \sqrt{U^2}$ on the discrepancy (7) from the resonant frequency ω_0 . Straight lines

$$\sqrt{U^2} = \pm \sqrt{\frac{\pi^2}{8} - 1} \left(\frac{\Delta}{\pi\epsilon}\right) \quad (44)$$

are separatrices. Below these lines the curves in Fig. 5 are constructed by the solution (37) for wave profiles which do not contain the shocks. Exactly on the lines (44) the Mach number M is equal to M_* and the transition to the discontinuous solution takes place. So, above the lines (44) another solution [Eq. (42)] was used for calculation of the frequency response.

As earlier, the Q -factor can be defined in two ways [see (31) and (32)]. The first definition leads to a formula analogous to (31):

$$Q_{NL} = \frac{c(\sqrt{U^2})_{\Delta=0}}{A} = \frac{c}{A} \sqrt{\frac{M}{\pi\epsilon}} = \frac{1}{\sqrt{M\pi\epsilon}}. \quad (45)$$

The second way gives the result

$$Q_{NL} = \frac{1}{\Delta} = \frac{\pi}{2\sqrt{2}} \frac{1}{\sqrt{M\pi\epsilon}}, \quad (46)$$

which differs slightly from (45).

The dependence $U_+(\Delta)$, where U_+ is the positive peak value of U , is shown in Fig. 6 by solid curves for the two

values of $M/\pi\epsilon$ equal to 0.25 and 0.09. The analytical expressions of the sections AB, BC, CD and DE of each curve are different. Namely, U_+ equals to

$$\begin{aligned} \frac{\Delta}{\pi\epsilon} - \sqrt{\left(\frac{\Delta}{\pi\epsilon}\right)^2 + C^2 - \frac{M}{\pi\epsilon}} & \quad (\text{AB}), \\ \frac{\Delta}{\pi\epsilon} + \sqrt{2} \sqrt{\frac{M}{\pi\epsilon} - \frac{\pi^2}{8} \left(\frac{\Delta}{\pi\epsilon}\right)^2} & \quad (\text{BC}), \\ -\frac{|\Delta|}{\pi\epsilon} + \sqrt{2} \sqrt{\frac{M}{\pi\epsilon}} & \quad (\text{CD}), \\ -\frac{|\Delta|}{\pi\epsilon} + \sqrt{\left(\frac{\Delta}{\pi\epsilon}\right)^2 + C^2 + \frac{M}{\pi\epsilon}} & \quad (\text{DE}). \end{aligned} \quad (47)$$

Here the eigenvalue C^2 is determined by Eq. (39). The straight lines 1 and 2 are the same separatrices as in Fig. 5. The line 3 separating sections CD and DE is described by

$$U_+ = \left(\frac{\pi}{2} - 1\right) \frac{\Delta}{\pi\epsilon}. \quad (48)$$

Note that U_+ is placed on the top of the shock front only for the section BC; for the other three sections U_+ belongs to smooth portions of the wave profile.

The maximum value of U_+ is located not at $\Delta = 0$, as a maximum in Fig. 5, but at some positive discrepancy:

$$\begin{aligned} (U_+)_{\max} &= \sqrt{2} \left(1 + \frac{4}{\pi^2}\right) \sqrt{\frac{M}{\pi\epsilon}}, \\ \left(\frac{\Delta}{\pi\epsilon}\right)_{\max} &= \frac{2\sqrt{2}}{\pi\sqrt{1 + \pi^2/4}} \sqrt{\frac{M}{\pi\epsilon}}. \end{aligned} \quad (49)$$

IV. STEADY-STATE VIBRATION IN A DISSIPATIVE MEDIUM AT HARMONIC EXCITATION

The problem considered in the preceding section is generalized here to a standing wave in a resonator filled with an absorbing medium. Such a problem setting is more complicated because derivatives of higher order appears in the wave equation due to nonzero dissipation $D \neq 0$. The analytical solution can be written in terms of known special functions only for harmonic motion of boundary. Fortunately, this case is most interesting for applications. The mathematical approach used here is similar to that developed by O. Rudenko²¹ to describe high-power hypersonic wave generated at Brillouin scattering. It was shown that the high-frequency acoustic wave excited by interacting laser beams is described by the Mathieu function

$$ce_0(z, q) \quad (50)$$

and its intensity is equal accurately to the characteristic value a_0 of the Mathieu function (50). This basic result was derived for a physical problem quite different from the concerned one. Moreover, it was published 30 years ago as a brief letter to the editor. That is why it is necessary to describe here some peculiarities of calculation and physical matter.

The standing waves in an absorbing layer ($D \neq 0$) must be studied on the base of differential equation (35). Using the transformation

$$U = \frac{2D}{\pi\epsilon} \frac{d}{d\xi} \ln W, \quad (51)$$

the nonlinear equation (35) of the first order is reduced to the linear equation of the second order:

$$\frac{d^2 W}{d\xi^2} - \frac{\Delta}{D} \frac{dW}{d\xi} = \left(\frac{\pi\epsilon}{2D}\right)^2 \left[C^2 + \frac{M}{\pi\epsilon} \cos \xi \right] W. \quad (52)$$

In particular, for zero discrepancy ($\Delta = 0$), the equation (52) can be transformed into the canonical form of the Mathieu equation:⁹

$$\frac{d^2 W}{dz^2} + \left[-\left(\frac{\pi\epsilon}{D}\right)^2 C^2 - \frac{\pi\epsilon M}{D^2} \cos 2z \right] W = 0, \quad z = \frac{\xi}{2}. \quad (53)$$

It is seen from Eq. (51) that the condition $\bar{U} = 0$ calls for the periodicity of the function W . Consequently, W can be written in terms of Mathieu functions.²³ The solution satisfying the transition to the linear limit ($M \rightarrow 0$) is

$$W = ce_0 \left(z, q = \frac{\pi\epsilon M}{2D^2} \right). \quad (54)$$

The intensity C^2 of the wave is determined by the characteristic value $a_0(q)$ of the Mathieu function ce_0 (50):

$$\bar{U}^2 = C^2 = -\left(\frac{D}{\pi\epsilon}\right)^2 a_0(q). \quad (55)$$

For weak excitation, using the two first terms of a series expansion²³ of a_0 for $q \ll 1$,

$$a_0 \approx -\frac{q^2}{2} + \frac{7q^4}{128}, \quad (56)$$

one can calculate \bar{U}^2 :

$$\bar{U}^2 = \frac{M^2}{8D^2} - \frac{7}{2048} \frac{(\pi\epsilon)^2 M^4}{D^6}. \quad (57)$$

The first term in (57) corresponds to the well-known linear result.

Using another asymptotic expansion for the characteristic value a_0 at $q \gg 1$,²³

$$a_0 \approx -2q + 2\sqrt{q} - \frac{1}{4} - \frac{1}{32\sqrt{q}}, \quad (58)$$

one can calculate the intensity for strong vibration of the boundary by means of (55):

$$\bar{U}^2 \approx \frac{M}{\pi\epsilon} - \sqrt{2} \frac{D}{\pi\epsilon} \sqrt{\frac{M}{\pi\epsilon}} + \frac{1}{4} \left(\frac{D}{\pi\epsilon}\right)^2 + \frac{1}{16} \left(\frac{D}{\pi\epsilon}\right)^4 \frac{\pi\epsilon}{M}. \quad (59)$$

An important characteristic of a resonator, its Q -factor, depends now on the absorption D :

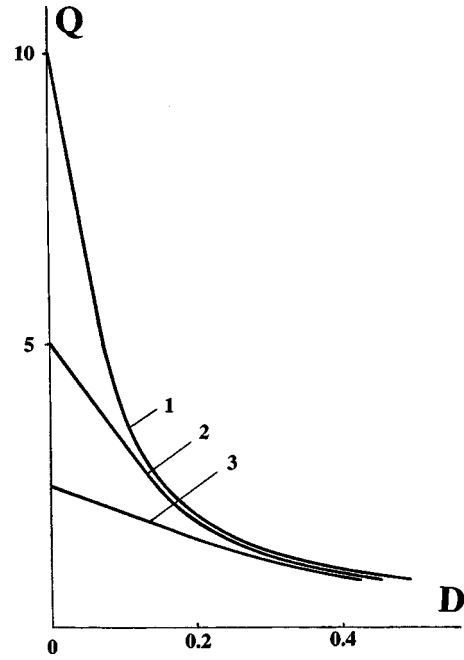


FIG. 7. Dependence of the Q -factor on the dimensionless dissipation D for three values of $\pi\epsilon M$ equal to 0.01, 0.04 and 0.16.

$$Q = \frac{1}{M} \sqrt{U^2} \approx \frac{1}{\sqrt{\pi\epsilon M}} \left(1 - \frac{\sqrt{2}}{2} d - \frac{1}{8} d^2 + \frac{\sqrt{2}}{16} d^3 + \frac{3}{128} d^4 \right),$$

$$d \equiv \frac{D}{\sqrt{\pi\epsilon M}}. \quad (60)$$

For $D=0$ the result (60) rearranges into the (45) for a non-dissipative medium.

For weak nonlinear distortion the quasi-linear Q -factor can be calculated on the base of Eq. (57):

$$Q = \frac{1}{2\sqrt{2}D} \left(1 - \frac{7}{512} \frac{1}{d^4} \right). \quad (61)$$

For $M \rightarrow 0$ or for $d \rightarrow \infty$ the equation (61) rearranges to the equation (33), valid in linear theory.

For arbitrary values of dissipation D the Q -factor equals to

$$Q = Q_{NL} \Psi(d = D Q_{NL}), \quad (62)$$

where the nonlinear Q -factor Q_{NL} is determined by Eq. (45) and $\Psi(d)$ is given by

$$\Psi(d) = \sqrt{-d^2 a_0 \left(q = \frac{1}{2d^2} \right)}. \quad (63)$$

The dependence of Q on D is shown in Fig. 7. The curves 1–3 are constructed by use of Eqs. (62) and (63) for three values of $\pi\epsilon M$ equal to 0.01, 0.04 and 0.16, correspondingly. Increase in the dimensionless dissipation number D , defined in Eq. (17), leads to decrease in the Q -factor. For small D -values the nonlinear absorption begins to play an important role for the decreasing of Q .

The analysis of the nonlinear frequency response calls for the solution to Eq. (52) at nonzero discrepancy, $\Delta \neq 0$. In

this general case the nonlinear equation (35) can also be reduced to a Mathieu equation. Instead of (51) we put

$$U = \frac{2D}{\pi\epsilon} \frac{d}{d\xi} \ln \left(w \exp \left(\frac{\Delta}{2D} \xi \right) \right). \quad (64)$$

Inserting (64) into (35) we obtain

$$\frac{d^2 w}{d\xi^2} = \left(\frac{\pi\epsilon}{2D} \right)^2 \left[C^2 + \left(\frac{\Delta}{\pi\epsilon} \right)^2 + \frac{M}{\pi\epsilon} \cos \xi \right] w. \quad (65)$$

It is still required that the mean value of U is zero. By use of (64) follows

$$\bar{U} = \frac{\Delta}{\pi\epsilon} + \frac{2D}{\pi\epsilon} [\ln w(\pi) - \ln w(-\pi)] = 0. \quad (66)$$

Consequently, w is not a periodic function and cannot be expressed through Mathieu functions.²³ Since the needed results cannot be found in Ref. 23 as well as in analogous tables, it is necessary to seek for an approximate solution to Eq. (35) or its linearized version (65).

For small Mach numbers M the mean intensity equals to

$$\bar{U}^2 = \frac{M^2}{8(\Delta^2 + D^2)} - \frac{(\pi\epsilon)^2 M^4}{512} \frac{7D^2 - 5\Delta^2}{(\Delta^2 + D^2)^3 (\Delta^2 + 4D^2)}. \quad (67)$$

In order to derive the result (67), the first four approximations were calculated in the solution of Eq. (35) by the method of successive approximations. This solution is described by very complicated formulas and is therefore not presented here.

For zero discrepancy ($\Delta=0$) the result (67) rearranges to form the result (57), obtained from the theory of Mathieu functions.

In the opposite limiting case, i.e., $q \gg 1$, the mean intensity depending on M , Δ and D for waves containing shocks can be calculated by another approach. The wave profile governed by Eq. (35) is found by the method of matched asymptotic expansions.^{25,26} This profile is presented as a sum of an “outer” solution, describing the smooth section of the profile, and an “inner” solution, describing the structure of a shock front of finite width. Thereafter, the averaging over the period of the square of this sum solution gives the intensity

$$\bar{U}^2 = \left[\frac{M}{\pi\epsilon} - \left(\frac{\Delta}{\pi\epsilon} \right)^2 \right] - \sqrt{2} \frac{D}{\pi\epsilon} \sqrt{\frac{M}{\pi\epsilon} - \frac{\pi^2}{8} \left(\frac{\Delta}{\pi\epsilon} \right)^2}. \quad (68)$$

At resonance, $\Delta \rightarrow 0$, the equation (68) reduces to the result (59) of the theory of Mathieu functions.

The calculation of the asymptotic ($q \gg 1$) solution described above is rather complicated. It contains features important for nonlinear perturbation theory and will be the subject of another work.

It follows from Eq. (68) that the nonlinear frequency response (solid curve 1 in Fig. 8) decreases with account for weak dissipation (dashed curve 2). Analogously, the linear frequency response (67), shown by the solid curve 3 in Fig. 8, decreases in its main part, with account for weak nonlinearity.

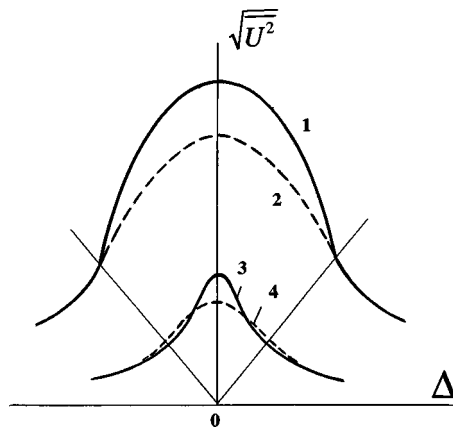


FIG. 8. Decrease in the nonlinear frequency response (curve 1) caused by weak dissipation (curve 2), and decrease in the linear frequency response (curve 3) with account for weak nonlinearity (curve 4)

V. DEVELOPMENT OF STANDING WAVES

Non-steady-state nonlinear vibrations in resonators have been studied much less than the stationary ones.^{11,12} The evolution equation (18) offers the possibility to study the transient process for any periodic motion of the boundary.

For the saw-tooth-like right-hand side of Eq. (18) considered in the beginning of Sec. III the non-steady-state solution at ($\Delta=0$) has a very simple form:¹²

$$U = - \sqrt{\frac{M}{2\epsilon}} \tanh \left(T \sqrt{\frac{\epsilon M}{2}} \frac{\xi}{\pi} \right), \quad -\pi \leq \xi \leq \pi. \quad (69)$$

The ratio of the root mean square particle velocity of the standing wave to the “amplitude” of the harmonic boundary vibration M tends, at $t \rightarrow \infty$, to the value Q_{NL} (31) calculated for steady-state vibration.

For a harmonic vibration of the boundary $x=L$ the right-hand side of Eq. (18) takes the form $(M/2)\sin \xi$. For this case the substitution (51) transforms (18) into the linear partial differential equation

$$\frac{\partial W}{\partial T} + \Delta \frac{\partial W}{\partial \xi} - D \frac{\partial^2 W}{\partial \xi^2} = - \frac{1}{2} q D \cos \xi W. \quad (70)$$

By the substitution

$$W = \exp \left(- \frac{1}{4} a D T \right) y(z), \quad z = \frac{\xi}{2}, \quad (71)$$

where a is a constant, the ordinary differential equation for the function $y(z)$ can be derived from (70):

$$\frac{d^2 y}{dz^2} - 2 \frac{\Delta}{D} \frac{dy}{dz} + (a - 2q \cos 2z)y = 0. \quad (72)$$

At zero discrepancy, $\Delta=0$, the equation (72) transforms into the canonical form of the differential equation for Mathieu functions. This is the resonant case, which can be studied in detail. The corresponding mathematical results were derived in Ref. 22 for another physical problem, but these results can be adopted for non-steady-state vibrations of resonators.

For zero initial condition $U(T=0, \xi)$ the solution of Eq. (70) can be written as a series of even Mathieu functions:

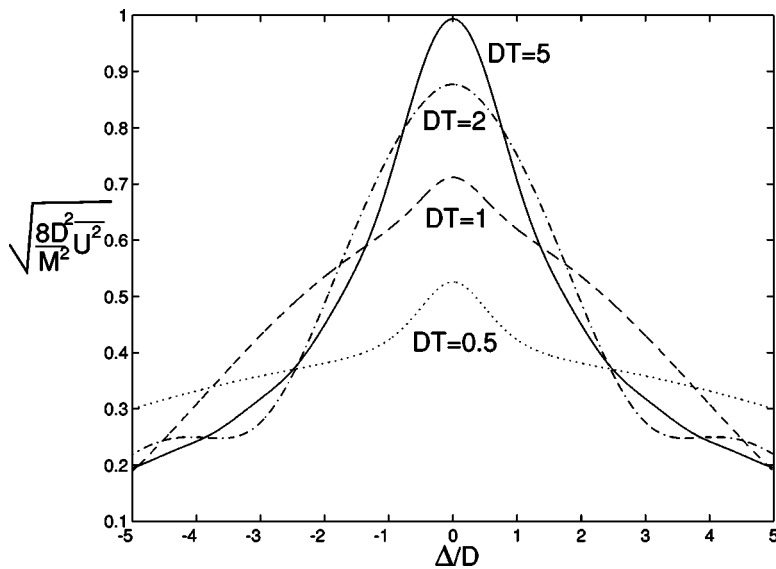


FIG. 9. Non-steady-state frequency response from Eq. (79) with $(\pi\epsilon M/2D^2) = 3$. Both nonlinearity and dissipation are taken into account.

$$W = \sum_{n=0}^{\infty} a_{2n} \exp\left[-\frac{1}{4}a_{2n}(q)DT\right] c e_{2n}\left(\frac{\xi}{2}, q\right), \quad (73)$$

where a_{2n} is given as

$$a_{2n} = \frac{\int_0^{2\pi} c e_0(\xi/2, q) d\xi}{\int_0^{2\pi} c e_{2n}^2(\xi/2, q) d\xi}. \quad (74)$$

The steady-state solution resulting from (73) and (51) at $T \rightarrow \infty$,

$$U = \frac{2D}{\pi\epsilon} \frac{d}{d\xi} \ln c e_0\left(\frac{\xi}{2}, \frac{\pi\epsilon M}{2D^2}\right), \quad (75)$$

coincides with the results (54) and (51) of Sec. V. For $q \gg 1$ the solution (75) takes the form

$$U = \sqrt{\frac{2M}{\pi\epsilon}} \left\{ \cos \frac{\xi}{2} - \frac{2 \exp(-2\sqrt{q}\xi)}{1 + \exp(-2\sqrt{q}\xi)} \right\}, \quad 0 \leq \xi \leq \pi, \quad (76)$$

and for $q \rightarrow \infty$ it does not depend on the linear absorption (i.e., on q) at all:

$$U = \sqrt{\frac{2M}{\pi\epsilon}} \cos \frac{\xi}{2} \operatorname{sgn} \xi, \quad -\pi \leq \xi \leq \pi. \quad (77)$$

The solution (77) coincides with (27) for $\Delta = 0$.

The increase in energy of resonator in the resonator can be studied on the base of solution (73) for zero discrepancy and by numerical methods only. Instead, it is possible to develop the theory for analytical description of the process of accumulation of acoustic energy. The approximate solution to inhomogeneous Burgers Eq. (18) is used here with account for all principal parameters: nonlinearity, absorption and discrepancy. This solution,

$$U = \frac{M}{2\sqrt{D^2 + \Delta^2}} \sin\left(\xi - \arctan \frac{\Delta}{D}\right) - \frac{M \exp(-DT)}{2\sqrt{D^2 + \Delta^2}} \sin\left[\xi - \Delta T - \arctan \frac{\Delta}{D} + \pi\epsilon TM\right] - \frac{\pi\epsilon TU}{2\sqrt{D^2 + \Delta^2}} \sin\left(\xi - \arctan \frac{\Delta}{D}\right), \quad (78)$$

is derived by the method of transition to implicit variable used many times earlier (see, for example, Refs. 13, 27, and 28). Calculations are rather complicated and therefore they are omitted here. As is shown in Ref. 27, solutions of the type (78) are of good accuracy in two limiting cases: at highly expressed nonlinear distortion of the wave profile, but in the region where a shock is yet not formed, or at weak nonlinearity, but at any T .

Using the solution (78), U^2 may be averaged over one period. The solution to this intricate problem is

$$\overline{U^2} = \frac{M^2}{8(D^2 + \Delta^2)} \left[1 - 2e^{-DT} \times \frac{2J_1(\pi\epsilon TM/[2\sqrt{D^2 + \Delta^2}e^{-DT}])}{(\pi\epsilon TM/[2\sqrt{D^2 + \Delta^2}e^{-DT}])} \cos(\Delta T) + e^{-2DT} \right]. \quad (79)$$

One can easily check the validity of this result at small values of M as the equation (79) for the acoustic energy in the cavity of the resonator turns into the corresponding linear solution.

In conclusion, the non-steady-state solutions to Eq. (18) are given here for weakly expressed nonlinear effects. Expand the periodic right-hand side of Eq. (18) in a Fourier series:

$$-\frac{M}{2} f(\xi - \pi) = \frac{M}{2} \sum_{n=1}^{\infty} (\alpha_n \cos n\xi + \beta_n \sin n\xi). \quad (80)$$

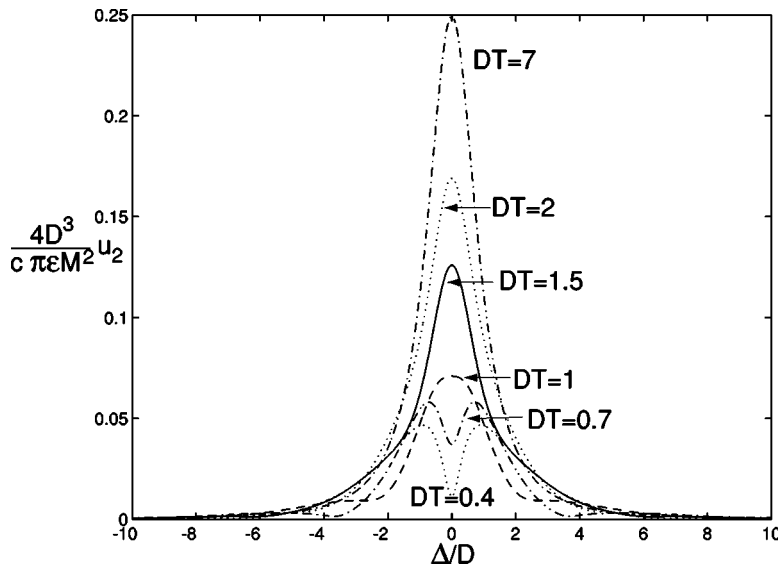


FIG. 10. Temporal evolution of the spectral line of the second harmonic [normalized amplitude versus discrepancy calculated from solution (84) and (85) with account for dissipative properties of the nonlinear medium].

The corresponding solution to Eq. (18) with the nonlinear term neglected equals

$$U = \frac{M}{2} \sum_{n=1}^{\infty} C_n [\sin(n\xi - \phi_n) - \exp(-n^2DT) \sin(n\xi - n\Delta T - \phi_n)], \quad (81)$$

where

$$C_n = \frac{1}{n} \sqrt{\frac{\alpha_n^2 + \beta_n^2}{\Delta^2 + n^2D^2}}, \quad (82)$$

$$\phi_n = \arctan \frac{\Delta\beta_n - nD\alpha_n}{\Delta\alpha_n + nD\beta_n}.$$

For example, at harmonic excitation ($\alpha_n=0$, $\beta_1=1$ and $\beta_n=0$ for $n \neq 1$), the standing wave has the same shape as the fundamental mode of (80):

$$\frac{u^{(1)}(x,t)}{c} = -\frac{M}{\sqrt{D^2 + \Delta^2}} \sin kx [\cos(\omega t - \phi_1) - \exp(-DT) \cos(\omega t - \phi_1 - \Delta T)]. \quad (83)$$

Using the linear solution (83), the nonlinear correction term is calculated by the successive approximation method:

$$\frac{u^{(2)}(x,t)}{c} = \frac{\pi\epsilon}{4} \frac{M^2}{D^2 + \Delta^2} \sin 2kx \sum_{m=1}^3 \Phi_m(t). \quad (84)$$

Here

$$\begin{aligned} \Phi_1 &= [(4D)^2 + (2\Delta)^2]^{-1/2} [\sin(2\eta - \phi_{1/2}) - \exp(-4DT) \sin(2\eta - 2\Delta T - \phi_{1/2})], \\ \Phi_2 &= -2[(3D)^2 + (3\Delta)^2]^{-1/2} [\exp(-DT) \sin(2\eta + \Delta T - \phi_1) - \exp(-4DT) \sin(2\eta - 2\Delta T - \phi_1)], \\ \Phi_3 &= [(2D)^2 + (4\Delta)^2]^{-1/2} [\exp(-2DT) \sin(2\eta + 2\Delta T - \phi_2) - \exp(-4DT) \sin(2\eta - 2\Delta T - \phi_2)], \end{aligned} \quad (85)$$

where $\eta = \omega t - \phi_1$. Evidently, the second approximation (84) corresponds to the second mode excited by nonlinear transfer from the fundamental mode.

The simple analytical expressions (83) and (84) offer a clear view of how the process of establishment of modes goes on at any dissipation D and discrepancy Δ . The increase in amplitudes, as well as the evolution of spectral lines (or “instantaneous” frequency response), can be analyzed for the first and second harmonics at small $M/\sqrt{D^2 + \Delta^2}$. A plot of the nonlinear correction term time evolution based on Eq. (85) is seen in Fig. 10.

VI. CONCLUSIONS

In order to increase the intensity of a standing wave, one has to enhance the Q-factor of the nonlinear resonator. As was shown above [cf. (31) and (32)], the limiting magnitude of Q is determined by nonlinear absorption caused by the formation of steep shock fronts.

Different methods have been suggested to suppress the process of shock formation. Zarembo *et al.*²⁹ suggest a resonator, of which one boundary has a frequency-dependent impedance; each reflection from this boundary introduces phase shifts between different harmonics destroying the front. Lawrenson *et al.*,⁶ Ladbury,³⁰ and Ilinskii *et al.*³¹ have realized the idea of controlling the waveform and phase shifts between harmonics using resonators of complex shape. Rudenko³² suggested the method of controlling nonlinear energy flows between harmonics by introducing selective absorbers, which can be used, in particular, to enhance the Q-factor by suppressing the “key” frequencies.³³ This method was realized experimentally,³⁴ but its possibilities are being studied up to now.^{35,36}

Quite another approach to enhance Q with no changes in the design of the resonator was suggested in Ref. 37. It was shown that the unfavorable effects of nonlinearity due to the movable boundary can be suppressed if the boundary executes a vibration of special form. More specifically, in order to provide harmonic vibration in the cavity, the resonator

must be excited by a periodic sequence of short “jerks” of its boundary.

If the usual linear Q -factor of a resonator is high enough, the significant acoustic energy can be accumulated in the cavity even if the source of the external pump of energy is weak. High-intensity vibration can easily be generated and nonlinear phenomena come into play. In particular, Q falls down, and, therefore, even strong increase in pump (energy inflow) leads to weak amplification of the standing wave. Definitions of frequency response by the relative rms of the acoustic field or by the maximum magnitude are given, suitable for different applications. Resonant curves illustrating nonlinear frequency response are constructed. The dependence of Q on the intensity of excitation and on linear properties are studied. Both wave profiles and energy characteristics for steady-state vibration and its development are analyzed. Different possibilities to enhance Q and the energy of acoustic vibration are discussed.

To analyze these phenomena, the analytic approach to high-intensity standing waves is used, based on nonlinear functional equations. The problem is radically simplified by separation of resonant and nonresonant nonlinear interactions, by introduction of small parameters and different temporal scales, and by reducing functional equations to differential ones.

¹A. B. Coppins and A. A. Atchley, “Nonlinear standing waves in cavities,” in *Encyclopedia of Acoustics* (Wiley, New York, 1997), pp. 237–246.
²M. A. Ilhamov, R. G. Zaripov, R. G. Galiullin, and V. B. Repin, “Nonlinear oscillations of a gas in a tube,” *Appl. Mech. Rev.* **49**, 137–154 (1996).
³O. V. Rudenko and S. I. Soluyan, *Theoretical Foundations of Nonlinear Acoustics* (Plenum, Consultants Bureau, New York, 1977).
⁴M. F. Hamilton and D. T. Blackstock (eds.), *Nonlinear Acoustics* (Academic, San Diego, 1997).
⁵V. B. Braginsky, V. P. Mitrofanov, and V. I. Panov, *Systems with Small Dissipation* (Chicago U.P., Chicago, 1985).
⁶C. C. Lawrenson, B. Lipkens, T. S. Lucas, D. K. Perkins, and T. W. van Doren, “Measurement of macroscopic standing waves in oscillating closed cavities,” *J. Acoust. Soc. Am.* **104**, 623–636 (1998).
⁷V. V. Kaner, O. V. Rudenko, and R. V. Khokhlov, “Theory of nonlinear oscillations in acoustic resonators,” *Sov. Phys. Acoust.* **23**, 432–437 (1977).
⁸V. V. Kaner, A. A. Karabutov, and O. V. Rudenko, “Nonlinear effects in acoustical resonators,” in *Nonlinear Acoustics* (Institute of Applied Physics Edition, Gorki, 1980) (in Russian), pp. 135–140.
⁹W. Chester, “Resonant oscillations in closed tubes,” *J. Fluid Mech.* **18**, 44–66 (1964).
¹⁰S. Temkin, “Propagating and standing sawtooth waves,” *J. Acoust. Soc. Am.* **45**, 224–227 (1969).
¹¹V. E. Gusev, “Buildup of forced oscillations in acoustic resonator,” *Sov. Phys. Acoust.* **30**, 121–125 (1984).
¹²O. V. Rudenko, C. M. Hedberg, and B. O. Enflo, “Nonlinear standing waves in a layer excited by periodic motion of its boundary,” *Acoust. Phys.* **47**, 452–460 (2001).
¹³V. P. Kuznetsov, “Equations of nonlinear acoustics,” *Sov. Phys. Acoust.* **16**, 467–470 (1971).
¹⁴C. Nyberg, “Spectral analysis of a two frequency driven resonance in a closed tube,” *Acoust. Phys.* **45**, 86–93 (1999).

¹⁵V. V. Kaner and O. V. Rudenko, “Propagation of waves of finite amplitude in acoustic waveguides,” *Moscow Univ. Phys. Bull.* **33**(4), ■–■ (1978).
¹⁶M. B. Vinogradova, O. V. Rudenko, and A. P. Sukhorukov, *Theory of Waves, 2nd edition* (Nauka, Moscow, 1990) (in Russian).
¹⁷A. A. Karabutov and O. V. Rudenko, “Nonlinear plane waves excited by volume sources in a medium moving with transonic velocity,” *Sov. Phys. Acoust.* **25**, 306–309 (1980).
¹⁸B. K. Novikov, O. V. Rudenko, and V. I. Timoshenko, *Nonlinear Underwater Acoustics* (American Institute of Physics, New York, 1987).
¹⁹V. E. Gusev and A. A. Karabutov, *Laser Optoacoustics* (American Institute of Physics, New York, 1993).
²⁰O. V. Rudenko and A. V. Shanin, “Nonlinear phenomena accompanying the development of oscillations excited in a layer of a linear dissipative medium by finite displacements of its boundary,” *Acoust. Phys.* **46**, 334–341 (2000).
²¹O. V. Rudenko, “Feasibility of generation of high-power hypersound with the aid of laser radiation,” *JETP Lett.* **20**, 203–204 (1974).
²²A. A. Karabutov, E. A. Lapshin, and O. V. Rudenko, “Interaction between light waves and sound under acoustic nonlinearity conditions,” *Sov. Phys. JETP* **44**, 58–63 (1976).
²³M. Abramovitz and I. A. Stegun, *Handbook of Mathematical Functions* (Dover, New York, 1970).
²⁴L. D. Landau and E. M. Lifshitz, *Fluid Mechanics* (Pergamon, London, 1959).
²⁵B. O. Enflo, “Saturation of nonlinear spherical and cylindrical sound waves,” *J. Acoust. Soc. Am.* **99**, 1960–1964 (1996).
²⁶M. Van Dyke, *Perturbation Methods in Fluid Mechanics* (Parabolic, Stanford, CA, 1975).
²⁷Yu. R. Lapidus and O. V. Rudenko, “New approximations and results of the theory of nonlinear acoustic beams” *Sov. Phys. Acoust.* **30**, 473–476 (1984).
²⁸O. V. Rudenko, “Interactions of intense noise waves,” *Sov. Phys. Usp.* **29**(7), 620–641 (1986).
²⁹L. K. Zarembo, O. Yu. Serdobol’skaya, and I. P. Chernobai, “Effect of phase shifts accompanying the boundary reflection on the nonlinear interaction of longitudinal waves in solids,” *Sov. Phys. Acoust.* **18**, 333–338 (1972).
³⁰R. Ladbury, “Ultrahigh-energy promise new technologies,” *Phys. Today* **51**, 23–24 (1998).
³¹Y. A. Ilinskii, B. Lipkens, T. S. Lucas, T. W. Van Doren, and E. A. Zabolotskaya, “A theoretical model of nonlinear standing waves in an oscillatory closed cavity,” *J. Acoust. Soc. Am.* **104**, 623–636 (1998).
³²O. V. Rudenko, “On the problem of artificial nonlinear media with resonance absorbers,” *Sov. Phys. Acoust.* **29**, 234–237 (1983).
³³O. V. Rudenko, “Nonlinear acoustics: progress, prospects and problems,” *Priroda (Nature)* **7**, 16–26 (1986).
³⁴V. G. Andreev, V. E. Gusev, A. A. Karabutov, O. V. Rudenko, and O. A. Sapozhnikov, “Enhancement of Q -factor of a nonlinear acoustic resonator by a selectively absorbing mirror,” *Sov. Phys. Acoust.* **31**, 162–163 (1985).
³⁵V. A. Khokhlova, S. S. Kashcheeva, M. A. Averkiou, and L. A. Crum, “Effect of selective absorption on nonlinear interactions in high intensity acoustic beams,” in *Nonlinear Acoustics at the Turn of the Millennium, Proceedings of ISNA 15*, edited by W. Lauterborn and T. Kurz, AIP Conf. Proc. **524**, 151–154 (2000).
³⁶O. V. Rudenko, A. L. Sobisevich, L. E. Sobisevich, and C. M. Hedberg, “Enhancement of energy and Q -factor of a nonlinear resonator with an increase in its losses,” *Dokl. Phys.* **47**, 330–333 (2002).
³⁷O. V. Rudenko, “Nonlinear oscillations of linearly deformed medium in a closed resonator excited by finite displacements of its boundary,” *Acoust. Phys.* **45**, 351–356 (1999).